LAWRENCE
LIVERMORE
NATIONAL
LABORATORY

UCRL-JRNL-226429

Hybrid atomic models for spectroscopic plasma diagnostics

S. B. Hansen, J. Bauche, C. Bauche-Arnoult, M. F. Gu

November 29, 2006

High Energy Density Physics

Hybrid atomic models for spectroscopic plasma diagnostics

S.B. Hansen [a,*] J. Bauche [b] C. Bauche-Arnoult [b] M.F. Gu [c]

[a] *Lawrence Livermore National Laboratory, P.O. Box 808, L-473,Livermore, CA 94550, USA*

[b] *Laboratoire Aimé Cotton, Campus d'Orsay, Bâtiment 505, 91405 Orsay, France*

[c] *Kavli Institute for Particle Astrophysics and Cosmology and Department of Physics, Stanford University, CA 94305, USA*

Abstract

We propose a hybrid approach to treating atomic structure and rates in collisional-radiative models, combining the completeness of highly averaged models with the accuracy of detailed models. The hybrid scheme supplements a small subset of coronally accessible fine structure levels with a complete set of configuration- and superconfiguration-averaged levels and produces spectra based on transitions among a mix of fine-structure and relativistic configuration-averaged levels. Convenient expressions are given for obtaining rates between the fine structure and averaged levels and a technique for propagating configuration interaction from the fine structure calculations to configuration averages is described. We present results from a trial hybrid model of germanium which demonstrate the accuracy of the hybrid model for charge state distributions and spectra.

Key words: Collisional-radiative, Non-LTE, Spectroscopic

1 Introduction

Collisional-radiative spectroscopic models are valuable diagnostic tools for a wide variety of plasmas. Their reliability is limited by two competing factors: 1) the detail and precision of the energy levels and rates used in the underlying atomic model, and 2) the completeness of that energy level structure and level coupling. The importance of the first component is clear: Emission

* Corresponding author: hansen50@llnl.gov

wavelengths, intensities, and the level populations obtained by solving a coupled set of collisional-radiative rate equations can be no more accurate than the underlying atomic data. The second component, completeness, is no less important. At low and moderate densities, accurate calculations require the inclusion of a large number of Auger channels and high Rydberg states to properly describe ionization balances and radiative cascades to metastable levels. At high densities, continuum lowering may reduce the maximum quantum number needed for accuracy, but can also greatly increase the number of accessible configurations in complex ions.

Highly complete models tend to rely on statistical atomic data and, while they perform well at high densities where collisions enforce local thermodynamic equilibrium (LTE), they can neither account for the kinetic effects of low-lying metastable levels nor reliably reproduce the spectra of closed-shell ions at low and moderate densities. In contrast, highly detailed models based on fine structure atomic data are reliable near closed-shell ions and at low densities but become intractable for complex ions. To bridge the gap between these two persistent categories of collisional-radiative models, we propose a hybrid approach to the level structure in which a small subset of detailed levels is augmented by a complete set of configuration- and superconfiguration-averaged levels.

The level structure of the proposed hybrid model is described with more precision in the following section. In Section 3, we describe various ways to obtain rates between hybrid levels. At this point, the hybrid model will give reliable charge state distributions and level populations with all the advantages of both detailed and averaged models. In Section 4, we discuss how one can also obtain spectroscopic-quality emission or absorption spectra by reconstituting highly averaged levels into relativistic configuration averages and approximating configuration interaction effects in transition arrays using information contained in the fine structure level subset. Finally, in section 5, we present results from a trial hybrid model of germanium.

2 Proposed hybrid model level structure

We begin with the observations that x-ray emission from closed shell ions and from even complex ions in the low-density coronal regime [1] is often very well described by models with a fairly restricted set of fine structure levels directly accessible via single electron transitions from the ground configuration. Such models work well whenever collisional excitation from the ground state is the dominant population mechanism and spontaneous decay is the dominant depopulation mechanism, with two important caveats: First, reliable coronal models must include configurations up to a sufficiently large quantum number

(usually $n = n_{valence}+ \approx 5$ is sufficient [2]) to adequately describe radiative cascades into metastable levels, which give rise to the familiar density-sensitive diagnostic emission lines [3]. Second, accurate calculations of charge state distributions in the coronal regime require the inclusion of many dielectronic recombination channels, often through doubly excited levels not accessible from the ground configuration. In practice, these recombination channels are often approximated using convenient tables given in the literature [4,5].

Since any model which makes claims of spectroscopic accuracy must be able to describe high resolution spectra from well characterized, low-density plasma sources, we set as the skeleton of our hybrid model a fairly restricted set of fine structure levels belonging to configurations which are directly accessible via single-electron transitions from the ground state. Using the 15-electron P-like ion as an example, we have:

- ground configuration:
  $1s^2 2s^2 2p^6 3s^2 3p^3$
- single excitations from the valence shell to $n \leq n_{valence} + 2$
  $1s^2 2s^2 2p^6 3s\ 3p^4$
  $1s^2 2s^2 2p^6 3s^2 3p^2 3d$
  $1s^2 2s^2 2p^6 3s^2 3p^2 4\ell$
  $1s^2 2s^2 2p^6 3s^2 3p^2 5\ell$
  $1s^2 2s^2 2p^6 3s\ 3p^3 3d$
  $1s^2 2s^2 2p^6 3s\ 3p^3 4\ell$
  $1s^2 2s^2 2p^6 3s\ 3p^3 5\ell$
- single excitations from the first inner shell to $n \leq n_{valence} + 1$
  $1s^2 2s^2 2p^5 3s^2 3p^4$
  $1s^2 2s^2 2p^5 3s^2 3p^3 3d$
  $1s^2 2s^2 2p^5 3s^2 3p^3 4\ell$
  $1s^2 2s\ 2p^6 3s^2 3p^4$
  $1s^2 2s\ 2p^6 3s^2 3p^3 3d$
  $1s^2 2s\ 2p^6 3s^2 3p^3 4\ell$

A model based on this set of configurations, which we shall call coronal, will give a reasonable description of major resonance lines from low-density sources such as tokamaks, electron beam ion traps, and many astrophysical plasmas.

Coronal models become unreliable at moderate or high densities or in the presence of a thermal radiation field, where collisional excitation from the ground level is no longer the dominant excitation mechanism and excited configurations can have populations that approach or exceed (because of their large statistical weights) the population of the ground configuration. Large populations in singly excited configurations in turn open new channels to multiply excited configurations. For example, the coronal configurations of the P-like ion described above would not account for strong dipole transi-

tions from $1s^2 2s^2 2p^6 3s\ 3p^2 3d^2$ to $1s^2 2s^2 2p^6 3s\ 3p^2 3d\ 4f$, which may be significant in moderate- or high-density plasmas. A reliable, general-purpose model therefore must include a more extensive set of configurations. We define these additional configurations using Layzer's complexes defined according to the occupation numbers of the n shells [6] with notation $(n)^N\ (n')^{N'}...$ denoting the full complement of possible configurations within a superconfiguration (SC).

The number and type of superconfigurations required for a reasonably complete model have been investigated by Peyrusse and co-authors in a previous work [7], where it was determined that including SCs with energies up to three times the ionization potential should be adequate for thermal plasmas. If non-thermal electrons are present, we may wish also to include excitation from the inner shells.

For this work, we consider the following modest set of superconfigurations, using the P-like ion again as an example:

- all configurations in the ground SC:
  $(1)^2(2)^8(3)^5$
- single excitations from the valence shell to $n \leq n_{valence} + 4$
  $(1)^2(2)^8(3)^4(4)^1$
  $(1)^2(2)^8(3)^4(5)^1$
  $(1)^2(2)^8(3)^4(6)^1$
  $(1)^2(2)^8(3)^4(7)^1$
- single excitations from the first inner shell to $n \leq n_{valence} + 2$
  $(1)^2(2)^7(3)^6$
  $(1)^2(2)^7(3)^5(4)^1$
  $(1)^2(2)^7(3)^5(5)^1$

For closed-shell ions, we also include double excitations from the valence shell to $n = n_{valence} + 1$. For general models, more extensive doubly and even triply excited SCs might be added to the list above to ensure completeness.

Figure 1 shows the number of fine structure levels and configurations in ions from H-like to Ar-like that result from this set of superconfigurations. Since we must solve a system of $N \times N$ coupled rate equations, where N is the total number of levels, it is clear that the number of fine structure levels becomes intractable as soon as we have more than two or three electrons in the M shell, The number of configurations, however, remains tractable, as does the number of coronal fine structure levels defined above.

Thus we arrive at our proposal for the hybrid level structure: from a set of SCs with sufficient completeness to describe the general non-LTE problem, we replace a subset of coronal configurations with fine structure levels. In this way, we combine the accuracy of the coronal approach for low densities and closed

shell ions with the completeness of an averaged-level approach at moderate and high densities, while restricting the computational effort required to a computationally tractable set of levels, as shown in Fig. 1.

While this scheme can be used with any atomic data source, we have based our investigations on data from the fully relativistic flexible atomic code (FAC) code [5]. FAC can operate in two modes, giving atomic structure and rate data for either fine structure levels or relativistic configuration averages. In the hybrid model level scheme, the highly accurate calculations of fine structure levels and rates are rapid because we include only a restricted set of levels. Calculations of the larger, more complete set of relativistic configurations and rates are also rapid, since they do not involve configuration interaction or level mixing and bypass a great deal of the angular momentum algebra required for fine structure levels.

Once we have obtained a complete set of relativistic configurations (RC) and rates from the FAC code, we replace the subset of relativistic coronal configurations with fine structure levels, then average the remaining RCs into non-relativistic configurations with energies given by:

$$E_C = \sum_{RC} (g_{RC} E_{RC}) / \sum_{RC} g_{RC} \tag{1}$$

Here, RC is an index running over all relativistic configurations in the non-relativistic configuration C.

Finally, following the results of [8], if there are more than $q \approx 500$ non-relativistic configurations in any superconfiguration, we average them into a single SC with energy

$$E_{SC} = \sum_{C} (g_C E_C) / \sum_{C} g_C \tag{2}$$

where the index C runs over all configurations in the superconfiguration SC.

3 Calculation of rates

With the calculation of the hybrid level structure described above, we obtain from FAC a complete set of rates among relativistic configurations ($RC \rightarrow RC'$) supplemented by a complete subset of rates among fine structure levels ($FS \rightarrow FS'$). Since we retain all of the fine structure levels, we must also retain all of the $FS \rightarrow FS'$ rates. We obtain configuration-to-configuration rates by

first integrating the the $RC \rightarrow RC'$ cross sections over electron and photon distribution functions, and then averaging the $RC \rightarrow RC'$ rates through:

$$\text{Rate}(C \rightarrow C') = \sum_{RC'} \frac{\sum_{RC} g_{RC} \text{Rate}(RC \rightarrow RC')}{\sum_{RC} g_{RC}} \tag{3}$$

Configuration to superconfiguration rates are given by:

$$\text{Rate}(C \rightarrow SC') = \sum_{C'} \text{Rate}(C \rightarrow C') \tag{4}$$

with the indices RC' and C' running over their parent ensembles. Note that the averaging given in Eqns. (3) and (4) and the averaging continuing below does not have to be statistical: it could include a Boltzmann factor with the real or effective temperature following the numerical procedure used in the code MOST [9], the code RADIOM [10], or using the analytic form given in Ref. [11].

The final question is how to treat the rates between fine structure levels and configurations. There are three possible approaches: We might calculate an entire set of fine structure levels and all rates coupling the coronal subset with the whole, and then average the $FS \rightarrow FS'$ rates to obtain $FS \rightarrow C'$ rates:

$$\text{Rate}(FS \rightarrow C') = \sum_{FS'} \text{Rate}(FS \rightarrow FS') \tag{5}$$

This, however, obviates a good part of the efficiency of the hybrid scheme. The second approach is to obtain approximate $FS \rightarrow C'$ rates by statistically decomposing the available $C \rightarrow C'$ rates from Eq. (3), ensuring that on reversal we regain $C \rightarrow C'$ rates which are averages over the initial levels and sums of the final levels of the $FS \rightarrow FS'$ rates:

$$\text{Rate}_{\text{stat}}(FS \rightarrow C') = \text{Rate}(C \rightarrow C') \tag{6}$$

and

$$\text{Rate}_{\text{stat}}(C \rightarrow FS') = \frac{g_{FS'}}{\sum_{FS'} g_{FS'}} \text{Rate}(C \rightarrow C') \tag{7}$$

with FS' running over all fine structure levels in C'.

This statistical approach is reasonable, but we can better preserve the individual character of the fine structure levels by defining an additional factor f for the fine structure to configuration rates using coefficients of Slater

integrals [12], such that $\mathrm{Rate}(C\alpha J \rightarrow C') = f\ \mathrm{Rate}_{\mathrm{stat}}(FS \rightarrow C')$. Let $C = (n\ell)^N(n'\ell')^{N'+1}$ and $C' = (n\ell)^{N+1}(n'\ell')^{N'}$ denote the initial and final non-relativistic configurations, respectively, and αJ be the fine structure term of configuration C. For electric dipole radiative transitions, we find:

$$f^{E1} = \frac{1}{2\ell_>}\left[\frac{(N'+1)}{(2\ell'+1)}\ell_> + C(G^1;\alpha J)\right]\frac{(4\ell+2)(4\ell'+2)}{(4\ell-N+2)(N'+1)} \tag{8}$$

where $C(G^1;\alpha J)$ is the coefficient of the Slater integral $G^1(n\ell, n'\ell';\alpha J)$ in the expansion of the total interelectronic-repulsion energy of the αJ level in terms of the Slater integrals and $\ell_>$ is the larger of ℓ and ℓ'. This expression is valid even for transitions with one or more spectator electrons in open subshells, and may be applied to collisional excitation and de-excitation in the Van Regemorter and Mewe approximations [13,14]. It may also be applied to photonionization and collisional ionization and their inverse processes, because these are all monoelectronic processes. This generalization is linked with the multipolar expansion of the inverse distance between a free electron and a bound electron [15].

Figure 2 gives a comparison of the f factors for electric dipole rates as calculated in the statistical approximation ($f = 1$), from Eqn.(8), and from the fully relativistic calculations from FAC. The agreement of Eqn.(8) with the full calculations is remarkable.

In a similar way, one can define f factors for electric quadrupole transitions. For such transitions, there are three cases, depending on the values of ℓ and ℓ':

$$f^{E2}_{\ell'=\ell} = \frac{(N'+1)C(G^2;A) - C(G^2;\alpha J)}{(N'+1)C(G^2;A) - C(G^2;B)} \tag{9}$$

with $C(G^2;A) = -\ell(\ell+1)/(2\ell-1)(2\ell+3)$

and $C(G^2;B) = C(G^2;A)N(N'+1)/(4\ell+2)$.

$$f^{E2}_{\ell'=\ell+2} = \frac{(N'+1)C(G^2;D) - C(G^2;\alpha J)}{(N'+1)C(G^2;D) - C(G^2;E)} \tag{10}$$

with $C(G^2;D) = -3(\ell+1)(\ell+2)/2(2\ell+3)(2\ell+5)$

and $C(G^2;E) = C(G^2;D)N(N'+1)/(4\ell+2)$.

The case $\ell' = \ell - 2$ can be obtained from Eqn.(10) after exchanging $n\ell$ and $n'\ell'$, and changing ℓ into ℓ', N into $(4\ell' - N' + 1)$, and N' into $(4\ell - N + 1)$.

Having obtained this hybrid level structure and a complete set of hybrid rates, the standard collisional-radiative rate matrix can be solved to obtain reliable populations and charge state distributions: Since the hybrid model retains some fine structure detail, it accounts for the important effects of ladder ionization from highly populated metastable levels at low densities. It describes the populations of those metastables reliably, since it includes a complete set of excited levels from which radiative cascades can populate metastable levels. And since we can afford a fairly complete set of doubly excited configurations using the hybrid scheme, we can also account for many of the important Auger channels that might only be approximated in standard low-density models.

4 Calculation of spectra

So far we have presented a hybrid model which should give reliable populations and charge state distributions from the coronal to the LTE regimes. We wish also, however, to have a diagnostic tool, and for this we need more than a small subset of fine structure levels complemented by configurations and superconfigurations. Previous investigations have shown that transition arrays between relativistic configurations are a reasonable representation of emission and absorption on complex ions, [16]. Since our original data set was based on relativistic configurations, and since FAC provides the necessary transition array energies and widths (following [17]), we can return to that level of detail with ease by simply reconstituting the relativistic configurations as individual levels.

This can be done most simply statistically by:

$$X_{RC} = (g_{RC} X_C) / \sum_{RC} g_{RC} \tag{11}$$

where X_C is the population of the non-relativistic configuration and the index RC runs over all relativistic configurations within the configuration C But as with the rates, a Boltzmann factor including an effective temperature might be introduced here, either from a numerical calculation following [9] (which could be iterated with the populations) or analytically following [11]. We may even be able to preserve the non-statistical properties of the relativistic configurations by tracking various line formation processes, as suggested by Rosmej in [18]

We emphasize that we run no risk of double-counting emission from fine structure levels and the relativistic configurations, since we have discarded all of the relativistic configurations duplicated by fine structure levels in the set of coronal configurations when constructing our energy level scheme.

Even with reliable populations and transition widths, the emission features arising between relativistic configurations will not be as accurate as those between fine structure levels, since configuration interaction (CI) is included only within each configuration in the relativistic configuration mode of the FAC atomic structure code. Because configuration interaction can have significant effects on both transition energies and strengths [19–21], its absence in transitions among the *RC* levels could degrade the diagnostic utility of spectra from the hybrid model.

Our solution is to appeal to the configuration interaction information encoded in the fine structure levels, which include CI effects among all of the coronal configurations. Since the coronal configurations are calculated twice (once as fine structure levels and once as relativistic configurations), we can directly compare the transition energies and strengths between fine structure levels in coronal configurations and the (previously discarded) transition energies and strengths of the relativistic configurations in the coronal set. The difference between the two calculations can be propagated to all $n\ell j \rightarrow n'\ell' j'$ transitions regardless of the arrangement of spectator electrons in the relativistic configurations. In this way we can extend (approximately) the accuracy of the fine structure calculations to the averaged levels of the hybrid model.

5 Results from hybrid Ge model

We have implemented the hybrid model described above in the collisional-radiative code SCRAM [2] based on FAC data for H- through Ar-like ions of Germanium. To test the accuracy of the hybrid model, we have made three additional models comprising the set of levels described schematically in Section 2:

- A complete set of relativistic configurations for H- through Ar-like Ge
- A fully detailed, fine-structure model of O- through Na-like Ge
- A fully detailed, fine-structure model of H- through Be-like Ge

Figure 3 shows the calculated average ion charge as a function of temperature from the hybrid model and compares it to the results of some models from the third NLTE code comparison workshop [22]. This figure shows that the hybrid model gives very reasonable results, as compared with a variety of other codes, over a wide range of $\langle Z \rangle$ and is *at least as* accurate as the model based on solely on relativistic configurations.

We find that the hybrid model is in fact *more* accurate than the straight relativistic configuration model by comparing the predictions of the two models for charge state distributions and level populations of the closed-shell Ne-like

ion with the results of the fully detailed, fine-structure model of O- through Na-like Ge. The comparison given in Fig. 4(a) shows that the relativistic configuration model predicts a lower population for the F-like ion at a temperature of 600 eV and a density of 10^{20}cm^{-3} than the hybrid and fine structure models, which agree quite well. The reason for the failure of the relativistic configuration model is shown in Fig. 4(b): since the RC model averages over the metastable levels in the $(2\ell)^7(3\ell)$ configurations, it underpredicts their populations and cannot account properly for ladder ionization from Ne-like to F-like Ge. This underprediction of the $(2\ell)^7(3\ell)$ populations will also lead to an underprediction of the $3\ell - 2\ell$ resonance line intensities in the Ne-like spectrum.

Finally, we test our proposed approximate extension of configuration interaction effects from the fine structure coronal configurations to the non-coronal relativistic configurations. Figure 5 shows a comparison of Li-like K-shell satellite emission at a temperature of 8 keV and an electron density of 10^{14}cm^{-3} The low-density, few-electron case should be a challenging region for the statistical component of the hybrid model. In this ion, configuration interaction shifts the $2p-1s$ transitions of the detailed level model by ≈ 20 eV. In the top figure, no CI correction has been applied to the non-coronal relativistic configurations of the hybrid model, and the shape of the satellite feature does not conform to that of the detailed fine-structure model. When a CI correction is applied to the non-coronal transitions, using information obtained by comparing fine structure and relativistic configuration transition energies within the coronal configurations, the non-coronal transitions are shifted to agree quite well with the emission feature of the fully detailed model.

6 Conclusions

We have described a novel scheme for combining the advantages of fine structure and averaged models for use in collisional-radiative modeling and spectroscopic diagnostics, and have demonstrated the quality of its results through comparisons with standard relativistic configuration and fine structure models.

Acknowledgements

The work of SH was performed under the auspices of the U.S. Department of Energy by University of California Lawrence Livermore National Laboratory under contract No. W-7405-Eng-48. Part of this work was done during the stay of JB and CBA at the Lawrence Livermore National Laboratory. They would like to thank the people of V Division for their warm hospitality.

References

[1] K.L. Wong, M.J. May, P. Beiersdorfer, K.B. Fournier, B. Wilson, G.V. Brown, P. Springer, P.A. Neill, C.L. Harris, Phys Rev Lett 90 (2003) 235001.

[2] S.B. Hansen, PhD Dissertation, University of Nevada, Reno (2003) p. 66.

[3] U. Feldman, J.F. Seeley, A.K. Bhatia, J. Appl. Phys. 58 (1985) 3954.

[4] P. Mazzotta, G. Mazzitelli, S. Colafrancesco, N. Vittorio, Astronomy and Astrophysics Supplement 133 (1998) 403.

[5] M.F. Gu, Astrophysical Journal 590 (2003) 1131.

[6] C. Bauche-Arnoult, J. Bauche, J Quant Spectrosc Radiat Transfer 71 (2001) 189.

[7] O. Peyrusse, C. Bauche-Arnoult, J. Bauche, Phys Plasmas 12 (2005) 063302.

[8] O. Peyrusse, C. Bauche-Arnoult, J. Bauche, J Phys B 38 (2005) L137.

[9] J. Bauche, C. Bauche-Arnoult, K.B. Fournier, Phys Rev E 69 (2004) 026403.

[10] M. Busquet, Phys Fluids B 5 (1993) 4191.

[11] S. B. Hansen, K.B. Fournier, C. Bauche-Arnoult, J. Bauche, O. Peyrusse, J Quant Spectrosc Radiat Transfer 99 (2006) 272.

[12] J. Bauche, C. Bauche-Arnoult, E. Luc-Koenig, J.F. Wyart, M. Klapisch, Phys Rev A 28 (1983) 829.

[13] H. Van Regemorter, Astrophys J 136 (1962) 906.

[14] R. Mewe, Astron Astrophysics 20 (1972) 215.

[15] R.D. Cowan, The Theory of Atomic Structure and Spectra (University of California Press, Berkeley, 1981) p. 565.

[16] J. Abdallah, H.L. Zhang, C. J. Fontes, D. P. Kilcrease, B.J. Archer, J Quant Spectrosc Radiat Transfer 71 (2001) 107.

[17] A. Bar-Shalom, J. Oreg, W.H. Goldstein, Phys Rev E 51 (1995) 4882.

[18] F.B. Rosmej, A. Calisti, J Quant Spectrosc Radiat Transfer 99 (2006) 548.

[19] J. Bauche, C. Bauche-Arnoult, M. Klapisch, P. Mandelbaum, J.L. Schwol, J Phys B 20 (1987) 1443.

[20] J. Oreg, W.H. Goldstein, A. Bar-Shalom, M. Klapisch, Phys Rev A 39 (1989) 4599.

[21] K.B. Fournier, S.B. Hansen, Phys Rev A 71 (2005) 012717.

[22] C. Bowen, R.W. Lee, Yu. Ralchenko, J Quant Spectrosc Radiat Transfer 99 (2006) 102.

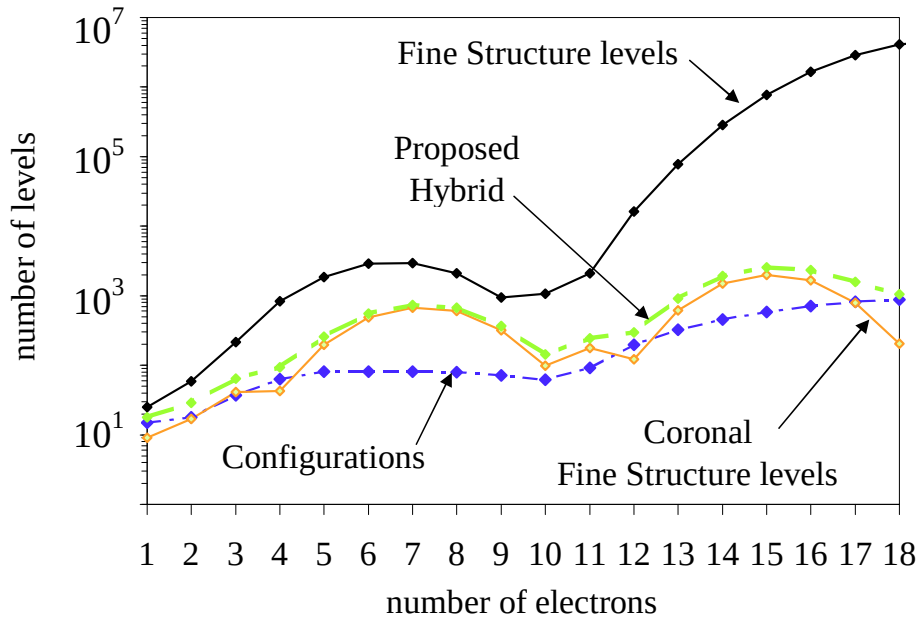

Fig. 1. Number of fine structure levels, coronal fine structure levels, configurations, and hybrid-model levels in the configuration sets described in the text for ions from H-like to Ar-like.

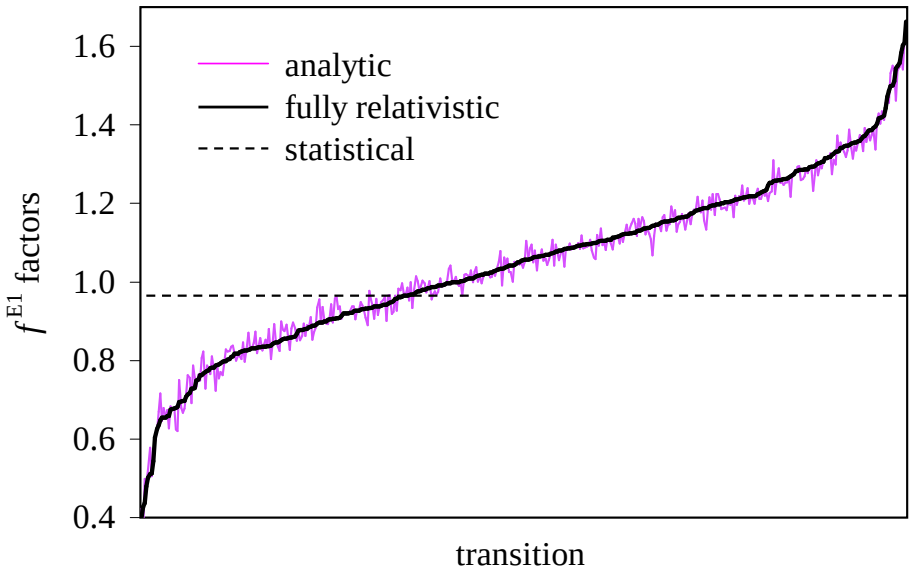

Fig. 2. Comparison of f^{E1} factors for Rate($p^2 d^4 \alpha J \rightarrow p^3 d^3$). The analytic formulation given in Eqn.(8) matches the fully relativistic level-to-level factors very well.

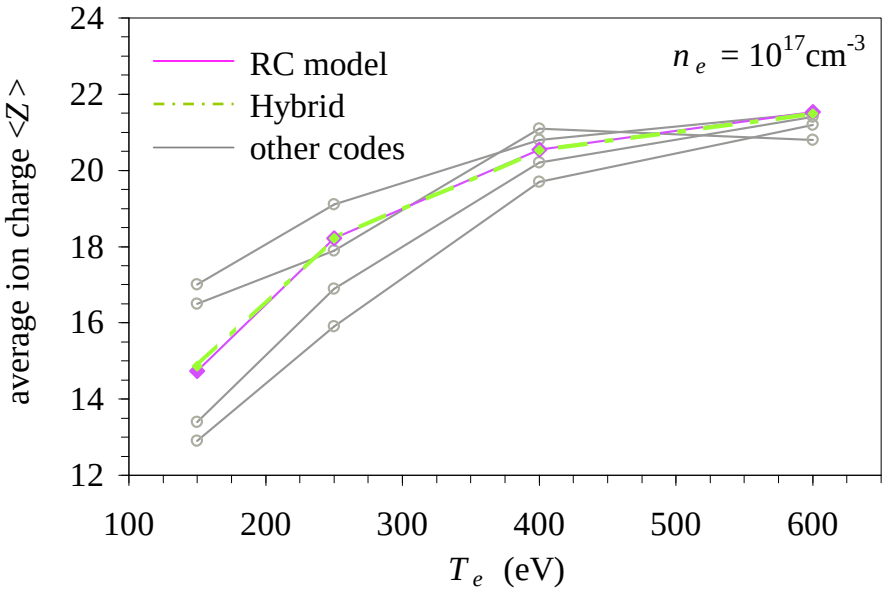

Fig. 3. Comparison of average ion charge calculations for Ge at $n_e = 10^{17}\text{cm}^{-3}$ from the hybrid model of the present work, a model based on relativistic configurations, and other codes (from Ref. [22])

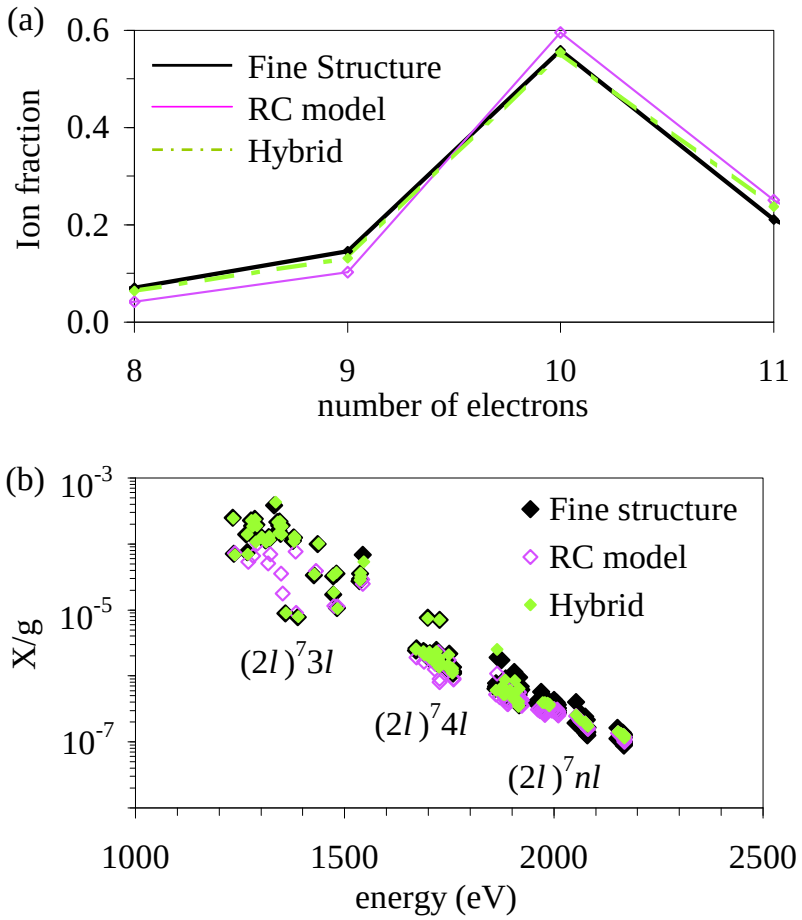

Fig. 4. (a) shows the charge state distribution of Ge ions at T_e=600 eV and $n_e = 10^{17}\mathrm{cm}^{-3}$ as calculated by the hybrid model and models based on relativistic configurations and detailed fine structure levels. (b) shows that the hybrid model agrees with the detailed models, in its predictions for the populations of metastable states in the $(2\ell)^7(3\ell)$ configurations, which the RC model underpredicts.

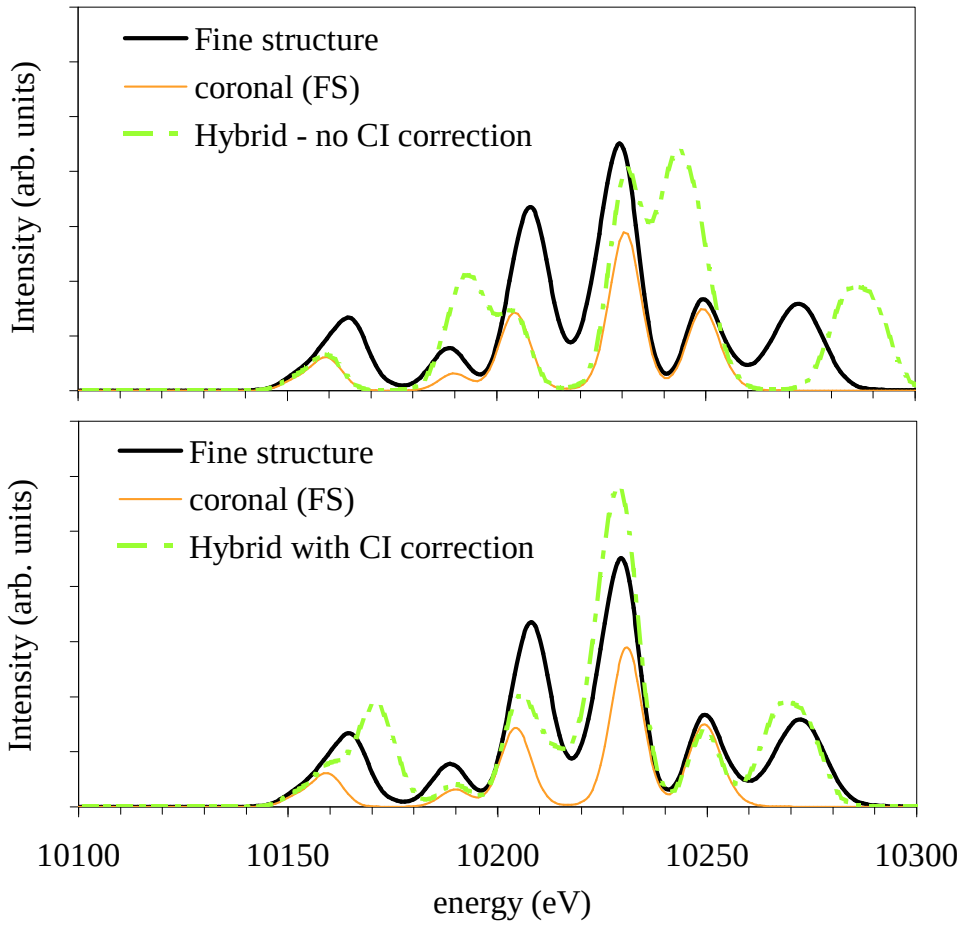

Fig. 5. Comparison of detailed fine structure model emission spectra of Li-like Ge at T_e=8 keV and $n_e = 10^{14}\mathrm{cm}^{-3}$ with the predictions of the hybrid model with and without approximate configuration interaction corrections to its relativistic configurations. Transitions among the coronal configurations are given by the dashed lines.